

Cross-Shelf Break Circumpolar Deep Water Intrusion in Shallower Area of Amundsen Sea

Ziang Li, Chuning Wang, Meng Zhou

School of Oceanography, Shanghai Jiao Tong University, Shanghai, China

Email: ziang.li_ocean@sjtu.edu.cn

How to cite this paper: Li, Z. A., Wang, C. N., & Zhou, M. (2024). Cross-Shelf Break Circumpolar Deep Water Intrusion in Shallower Area of Amundsen Sea. *Journal of Geoscience and Environment Protection*, 12, 115-127.

<https://doi.org/10.4236/gep.2024.124008>

Received: March 6, 2024

Accepted: April 27, 2024

Published: April 30, 2024

Abstract

The ice shelves of the Amundsen Sea are currently undergoing a rapid melting phase, making a significant contribution to the rise of sea level. The heat of melting was mostly provided by the Circumpolar Deep Water (CDW) from outside the continental shelf which can be transported southward by deep sea troughs on the continental shelf. There are three major troughs in Amundsen Sea, and current research on cross-shelf break CDW intrusion has focused on the locations where troughs connect to the shelf break. We recently found an unreported intrusion site at shelf break away from deep troughs, and the significant CDW intrusion signal in this shallow area near 106°W was captured by observed temperature data in World Ocean Database (WOD). The tendency of CDW intrusion southward in this site was verified by numerical particle tracking experiments. The temperature transport of this intrusion pathway was compared with a recognized pathway in troughs, and results suggested that they have a similar amount of heat contribution. However, numerical experiments modeling climate change indicated that the intrusion here is not as sensitive to westerly winds as in the troughs. Thus, although there is a significant amount of heat contribution in shallow area pathway, unlike deep troughs, where CDW intrusion into the ice shelves will increase under the climate change.

Keywords

Amundsen Sea, CDW Intrusion, Climate Change, Heat Transport

1. Introduction

The Amundsen Sea is located in the West Antarctic, where the ice shelves are in a phase of rapid melting. The total melting of the ice shelves in Amundsen Sea could raise global sea levels by 1.5 meters (Vaughan, 2008). The heat to melt the

ice shelves comes from the Circumpolar Deep Water (CDW) outside the continental shelf (Jacobs et al., 1996; Walker et al., 2007). CDW is the largest water mass in the global ocean, and it has high-temperature and high-salinity characteristics with potential temperature of $1.6^{\circ}\text{C} - 2.0^{\circ}\text{C}$ and salinity exceeding 34.6 PSU (Walker et al., 2013). Troughs across the continental shelf are able to transport the CDW southward continuously to the vicinity of the ice shelves. There are three major troughs in the Amundsen Sea (**Figure 1**), the (Western Trough) WT, (Central Trough) CT, and (Eastern Trough) ET; the WT connecting to the Dotson-Getz Trough (DGT), and the CT and ET converging to form the Pine Island Trough (PIT) on their southern side. The heat transported by the PIT to the Pine Island Ice Shelf (PIIS) and Thwaites Ice Shelf (TIS) can cause their basal melting rate to reach $4.3\text{-}17.7\text{ m year}^{-1}$ (Rignot et al., 2013). The maximum depths of all three troughs exceed the depth of the shelf break (700 m) (Nakayama et al., 2018), and most previous studies of CDW intrusions have focused only on these major troughs. In this study, a CDW intrusion site in the Shallow Area (SA, near 106°W) was found by the observations in the World Ocean Database (WOD) (Boyer et al., 2018) and the maximum depth of this area is $\sim 550\text{ m}$.

Previous observations have found that the CDW tends to intrude across the shelf break on shore near the troughs, which is related to the interaction of topography and currents (Thoma et al., 2008; Walker et al., 2013). However, it is not known whether such a dynamical mechanism exists in shallow water regions. Previous studies have suggested that CDW intrusion across the shelf

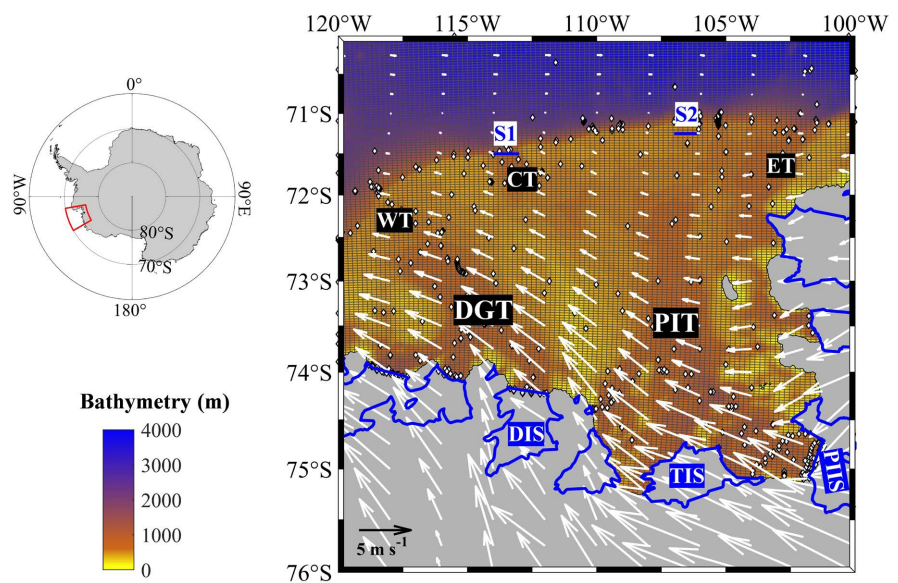


Figure 1. Bathymetry of the Amundsen Sea and its vicinity. WT, CT, ET, DGT, PIT, DIS, TIS and PIIS denote the locations of Western Trough, Central Trough, Eastern Trough, Dotson-Getz Trough, Pine Island Trough, Dotson Ice Shelf, Thwaites Ice Shelf and Pine Island Ice Shelf, respectively. The superimposed white arrows represent climatological annual mean wind fields. Small white diamonds represent the profiling locations of CTD stations.

break is a southward deflection of an eastward undercurrent on the continental slope (Assmann et al., 2013; Walker et al., 2013), and the formation of the undercurrent is related to the strength of the westerly winds in the Amundsen Sea (Steig et al., 2012). With the global climate change, there is a tendency for the westerlies to move southward (Armitage et al., 2018; Holland et al., 2019), which may lead to stronger CDW intrusion in the troughs of Amundsen Sea (Azaneu et al., 2023). However, the sensitivity of intrusion to climate change in SA has not been predicted yet.

In order to characterize the CDW intrusion in SA and measure its heat contribution to the shelf, a global reanalysis dataset was used; and a three-dimensional, high-resolution ocean model was built for exploring the response of CDW intrusions under the climate change. The descriptions of dataset and model are in Section 2. In Section 3, we verified the existence of the intrusion in SA near the shelf break through the numerical particle tracking experiments and compared the heat contributions in the trough and SA. We then modeled the variation in CDW intrusion under climate change. More discussions about bathymetry data in SA were discussed in Section 4; and conclusions were presented in Section 5.

2. Materials and Methods

2.1. *In-Situ* Measurements and Reanalysis Product

The *in-situ* measurements were obtained from the World Ocean Database (WOD) (Boyer et al., 2018). In the study area (120°W - 100°W) of Amundsen Sea, there are total 21,754 profiling casts, 608 of which are CTD casts (as shown in **Figure 1**). All the profiles contain more than a million potential temperature-salinity (θ - S) data pairs. The reanalysis product used in this study are provided by the Global Ocean Reanalysis Multi-Model Ensemble Products (GREP), which contains four sets of global reanalysis data, C-GLORS (hereinafter CGLO), FOAM-GLOSEA5v13 (hereinafter FOAM), GLORYS2V4 (hereinafter GLOR) and ORAS5 (hereinafter ORAS). The uniform horizontal resolution of them is 0.25° in all 75 levels over each vertical column. In order to compare to a best one that is closest to reality among the four sets, the θ - S data of reanalysis products were interpolated to the sampling positions of all CTD casts and the Taylor diagram (Taylor, 2001) was plotted for comparison (**Figure 2**). It is found that FOAM is the closest product to the observation measurements under any indicators.

To validate further the accuracy of FOAM's simulation of θ - S , the horizontal distributions of FOAM reanalysis and WOD observation data are shown in **Figure 3**. We calculated the maximum of time-averaged θ and S in the depths deeper than 300 m, where the most CDW is located (Wählén et al., 2012; Walker et al., 2013), from 1993 to 2019 in FOAM. Similarly, the maximum value of θ and S for each profile (deeper than 300 m) in WOD data were selected; to minimize overlap, 10% of the sampling points were randomly shown in **Figure 3**. For comparison, the WOD data were scattered on the coloring maps of FOAM. Even

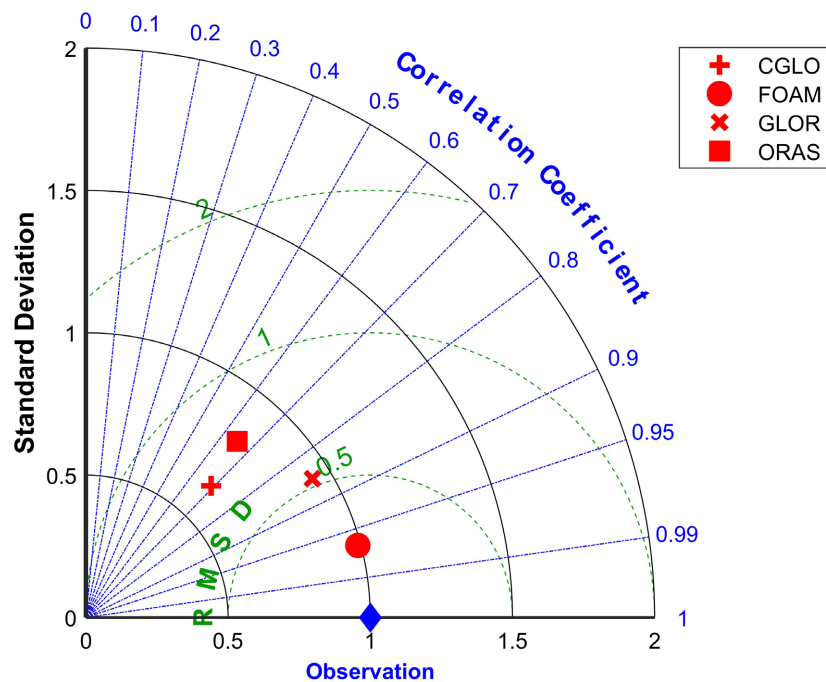


Figure 2. The Taylor diagram of reanalysis products and observation (CTD) measurements.

if the simulations of FOAM are biased in central areas, it is still accurate in troughs; and the θ - S tendency of FOAM and WOD along latitude and longitude are almost identical.

2.2. Numerical Model

The numerical investigation in this study is performed using the Regional Ocean Modelling System (ROMS) (Haidvogel et al., 2008; Shchepetkin & McWilliams, 2005); based on which a coupled sea ice-ice shelf-ocean general circulation model was developed (Wang et al., 2024). The average horizontal resolution of this model is ~ 6 km of the grid meshes in all 50 layers; more detailed model description and verification can be found in Wang et al. (2024). In this study, the climatological outputs of two numerical tests were used to compare variations in CDW intrusion at different area. The tests simulated climate change by enhancing westerly winds; and the detailed description and results are shown in Section 3.3.

3. Results

3.1. CDW Intrusion in Shallow Area

The cross-shelf break CDW intrusions in Amundsen Sea have been well-studied near the troughs, which were considered the main CDW intrusion pathways (Kim et al., 2021; Lars & Isabella, 2021; Wåhlin et al., 2010). However, an observed high-temperature, high-salinity signal at shelf break, away from the deep troughs, was captured in WOD data. As shown in **Figure 4**, there are clear CDW

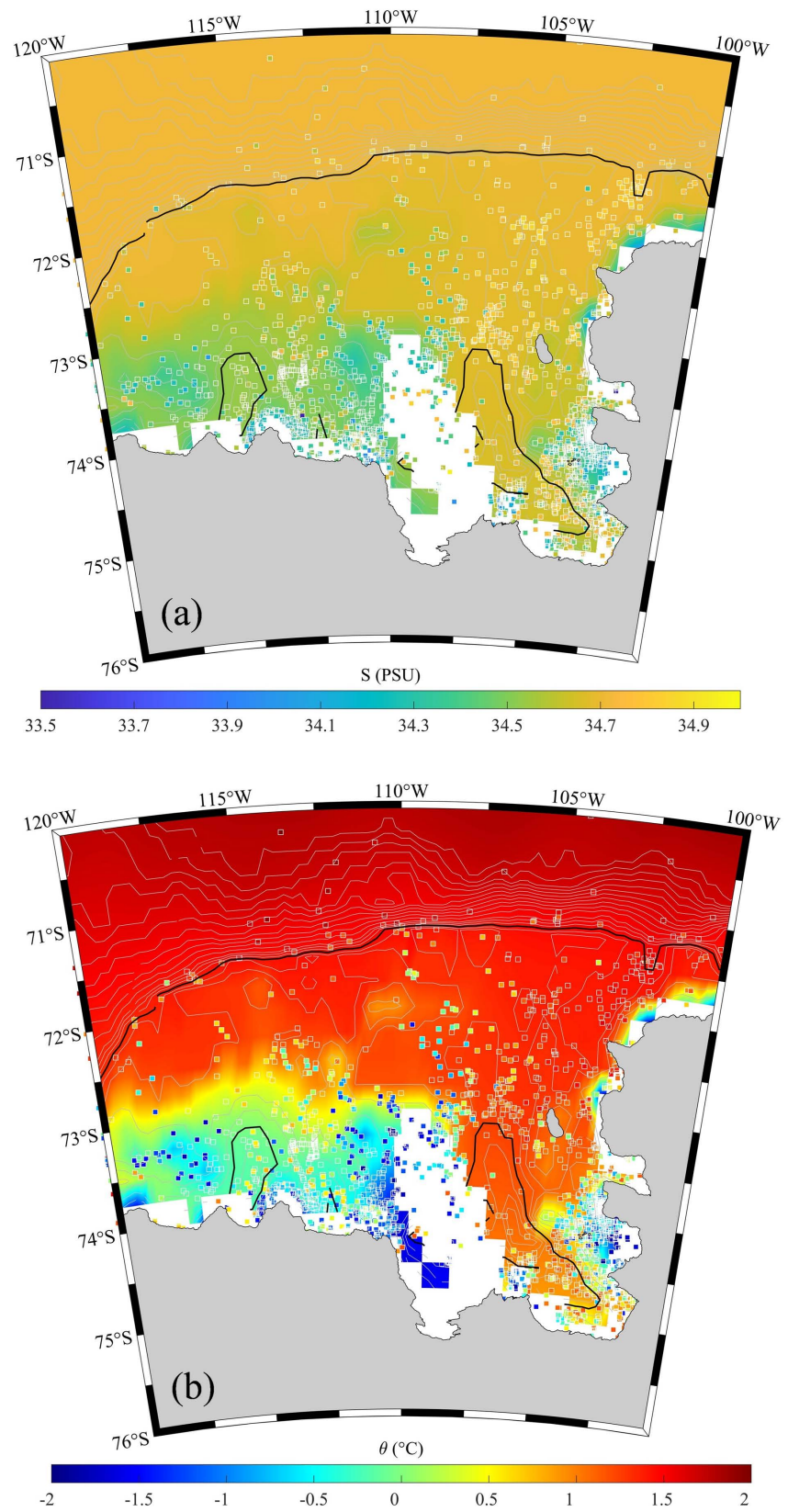


Figure 3. The horizontal comparison of (a) salinity and (b) potential temperature between FOAM and WOD data. The black lines represent the 700 m isobaths.

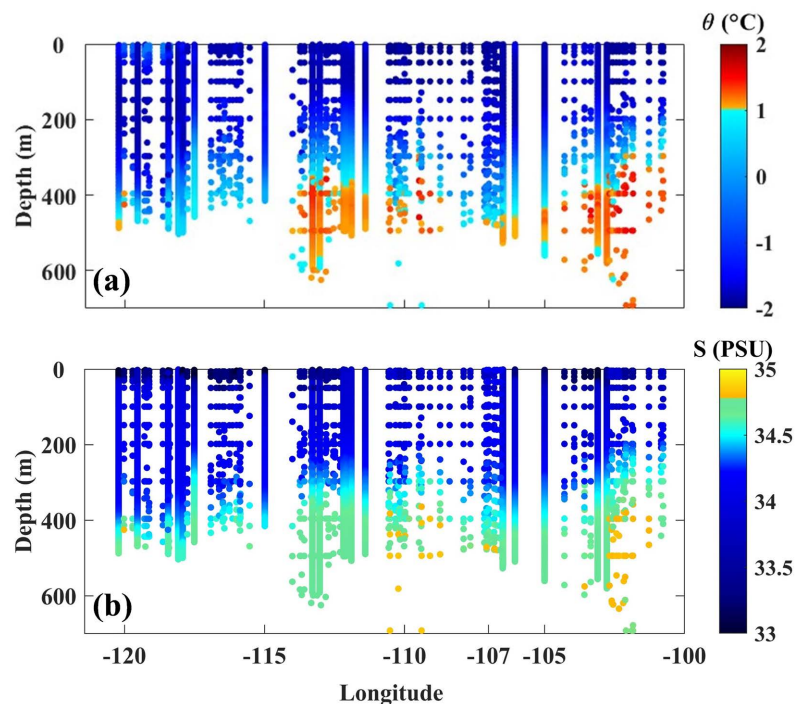


Figure 4. The distributions of (a) potential temperature and (b) salinity along the shelf break on the shelf side in WOD data.

intrusions at the locations (near 118°W , 113°W and 102°W) near the three major troughs WT, CT and ET. Although there is no deep-water trough in the vicinity of 106°W , CDW signals have also been observed there. Due to the lack of observed flow velocity data near 106°W , in order to further validate the existence of this intrusion site in SA, numerical particle tracking experiments were implemented through the FOAM.

As shown in **Figure 5**, the numerical particle tracking experiments were implemented at depth 300 m and 400 m. 11 particles were released at intervals of 0.1° on the slope at 106°W - 107°W . Some of particles were transported along the isobath to the east, and eventually they are transported by the ET to the south. Meanwhile, it is clearly found that there are many particles across the shelf break in SA, and they could be transported in the PIT within 9 months. Due to the PIT is connect to the ice shelves, the CDW intrusions in the SA also have a chance to reach the vicinity of the ice shelves.

3.2. Heat Transport in Shallow Area

Both observations and reanalysis product indicate that there are CDW intrusions in SA of Amundsen Sea. In order to weigh the heat contribution of in SA and compare the differences of heat contributions between SA and deep trough area, two zonal sections (S1 and S2 in **Figure 1**) were selected and the onshore temperature transport (TT) across the sections was calculated. As shown in **Figure 6(a)**, **Figure 6(b)**, it is suggested that S1 has the higher temperature than S2 and there is a shorter duration of the cold period ($\theta < 1.6^{\circ}\text{C}$) and a longer duration

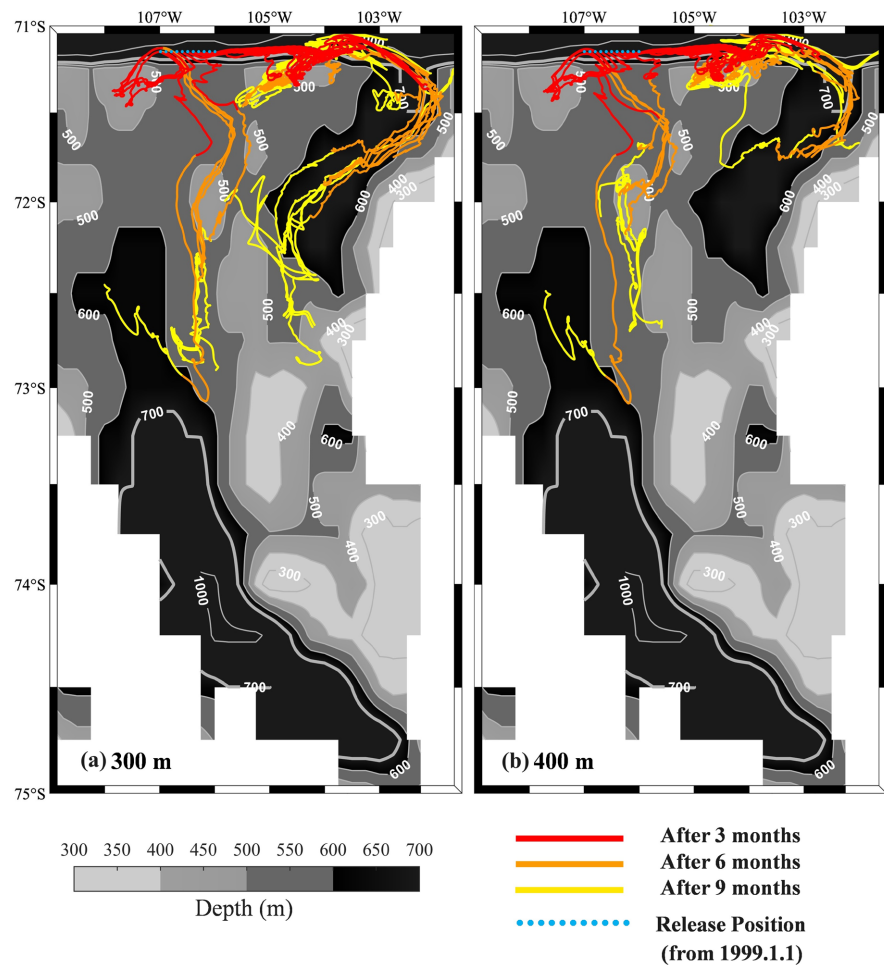


Figure 5. Pathways of particles at (a) 300 m and (b) 400 m on the shelf in the numerical particle tracking experiment. The red, orange and yellow lines are the particle's position after three, six and nine months, respectively. Blue points donate the particle release locations; gray lines are the isobaths.

of warm period ($\theta > 1.8^{\circ}\text{C}$) at section S2. Shifts in cold and warm periods in 2015 may be associated with El Niño events (Azaneu et al., 2023). As **Figure 6** (c) shows, in year 2010-2019, there is the same magnitude of the temperature transport (negative value represents onshore transport) in S1 and S2. And it is clearly found that the heat contribution to the shelf of SA is more than that of CT during the most time after year 2016; in this period, the mean temperature transport of SA is 3.9 times as large as which of CT. Thus, the heat contribution into Amundsen Sea continental shelf of SA cannot be ignored.

3.3. CDW Intrusion Variations under Climate Change

As **Figure 1** shows, the zonal winds in the Amundsen Sea are westerly winds outside the continental slope; and with the movement of the westerlies and the Amundsen Low under the climate change, the westerly winds have a tendency to increase (Schneider et al., 2015; Thoma et al., 2008; Thompson et al., 2011). Since westerly winds are a potential driver of CDW intrusions (Assmann et al., 2013;

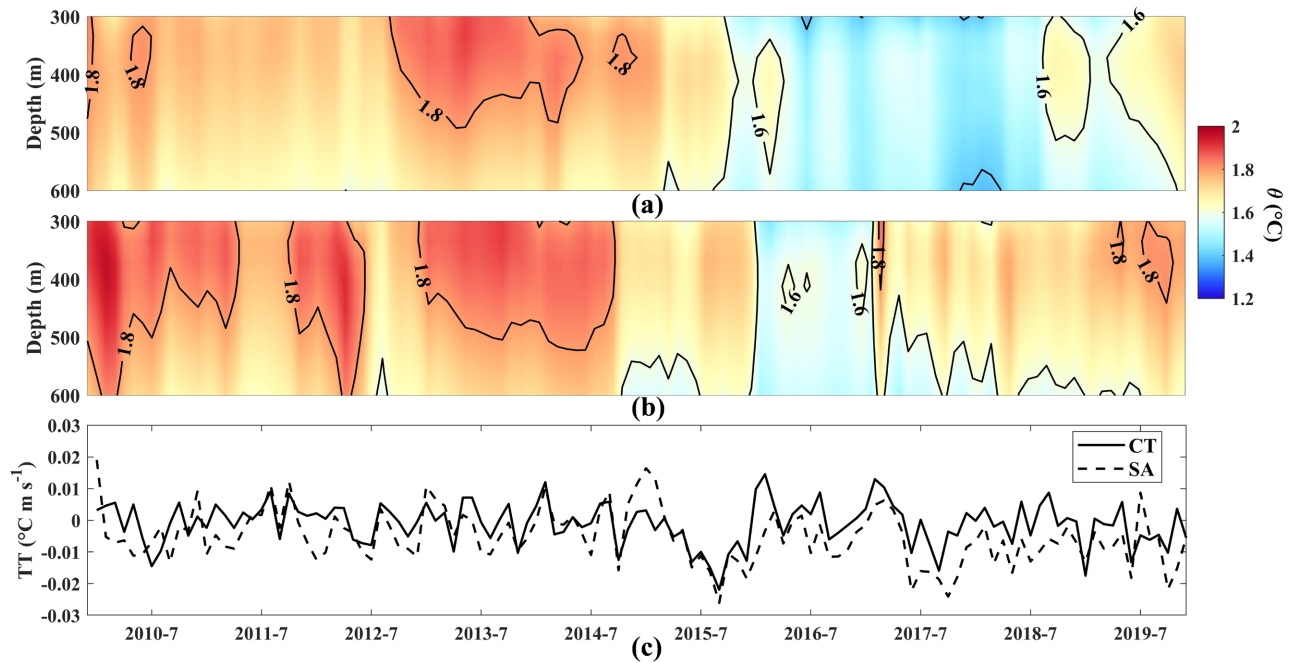


Figure 6. Potential temperature and temperature transport near the shelf break in shallow area and deep trough area. (a) Potential temperature at section S1; (b) Potential temperature at section S2; (c) Time series in year 2010-2019 of temperature transport ($TT = \theta u^{\perp}$, u^{\perp} is the cross-section flow velocity) in section S1 (near 106°W in SA) and S2 (in CT).

Steig et al., 2012), predicting the intrusions in SA and deep trough area under climate change is meaningful. We did two sets of numerical tests; as the control group, Test 0 provided the climatological results in one year; as an experimental group, Test 1 simulated the situation under climate change by adding 3 ms^{-1} westerly winds to the test area (67°S - 72°S , 130°W - 100°W). The results of two tests are shown in **Figure 7**.

The averaged climatological zonal winds in test area of Test 0 and Test 1 are shown in **Figure 7(a)**. Due to the spin up of model, the results of the first two months of the outputs are not analyzed. As **Figure 7(b)**, **Figure 7(c)** shows, the strength of the cross-section flow is stronger in Test 1 than in Test 0 in the most of time. To further quantify the intrusion, cross-section volume transport Q was calculated:

$$Q = \int_{-H}^{\eta} \int_{x_1}^{x_2} u^{\perp} dx dz. \quad (1)$$

where η is the sea surface height; H is the seabed depth; u^{\perp} is the cross-section flow velocity. As shown in **Figure 7(d)**, the monthly results suggested that Q is significantly larger for Test 1 than Test 0 in all months except for in October, when they were close to each other, suggesting that the CDW intrusion in CT tends to strengthen under the climate change. However, the intrusion in SA is not sensitive to the variations of the westerly winds. As **Figure 7(e)** & **Figure 7(f)** shows, the flow velocity remained almost unchanged between the results of Test 0 and Test 1. Only in July was there a significant increase in on shore transport, as **Figure 7(g)** shows, but this was due to increased outflow on the

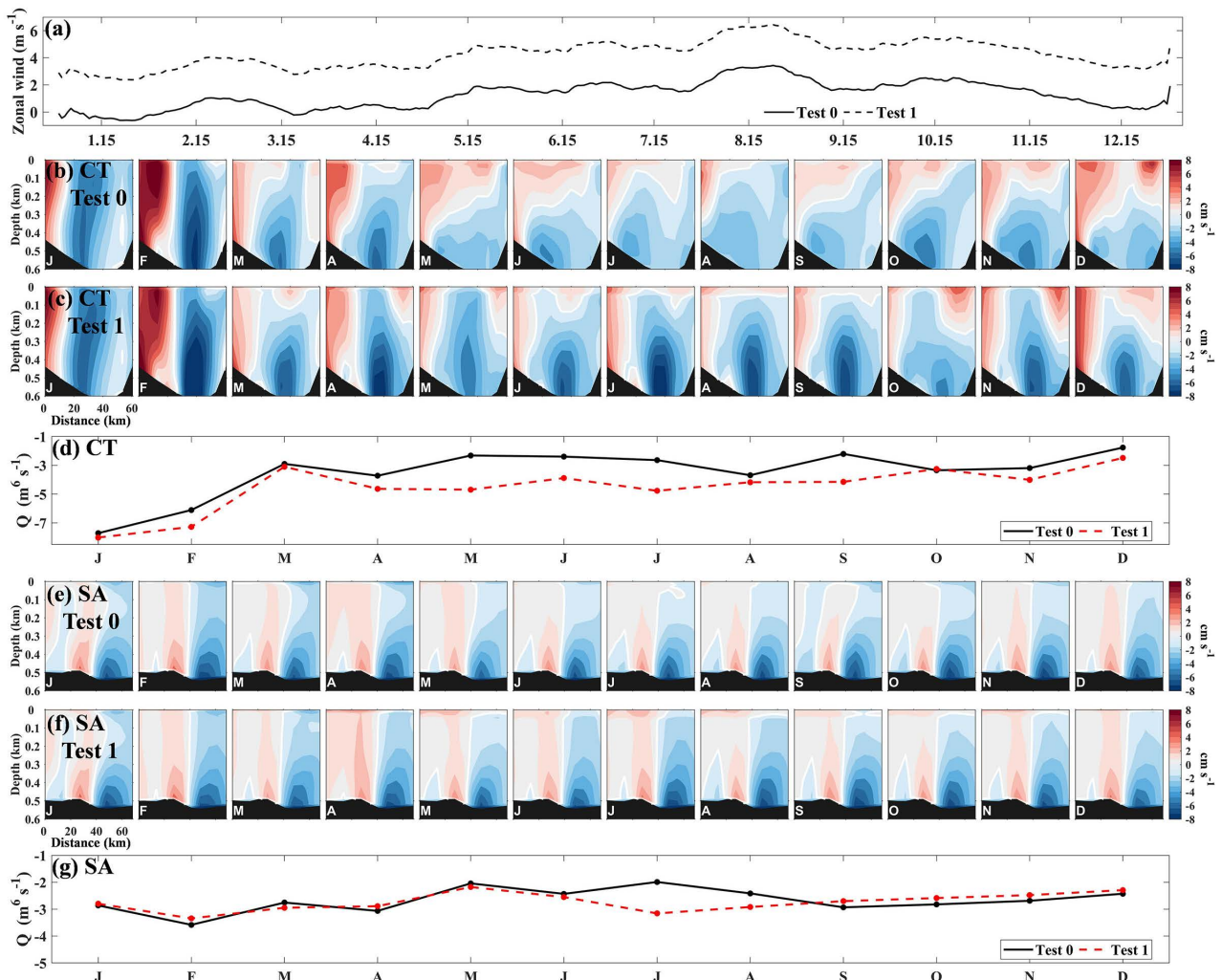


Figure 7. The results of numerical tests. (a) Window averaged zonal wind speed of two tests using 30-day window size in test area; The outputs of flow velocity in CT of (b) Test 0 and (c) Test 1; and the blue color represents the onshore direction; (d) The averaged volume transport Q of the section in CT, and the negative values represent the on shore direction; (e)-(f) Similar to (b)-(d), for the section in SA near 106°W .

surface, not stronger bottom intrusion. Thus, in our model results, the CDW intrusion in shallow area seem to be unaffected by the variations of westerly winds.

4. Discussion

We noticed a CDW intrusion site near the shelf break in the shallow area in WOD potential temperature data, and the intrusion site was also found in reanalysis product and model outputs. Due to the cross-isobath transport affected by the topography, different bathymetry data used in models or reanalysis products have different effects on the simulation results at the shelf break. Thus, comparison of the bathymetry data in models and reanalysis products is valuable in verifying the existence of this unreported intrusion site. Therefore, for comparison, the raw bathymetry data of ETOPO 1 (last modified: 2008-07-28; <https://www.ngdc.noaa.gov/mgg/global/relief/ETOPO1/data/>) which was used

in the assimilation of reanalysis product FOAM was downloaded; and the raw bathymetry data of BedMachine Antarctica v3 (last modified: 2022-10-11; <https://nsidc.org/data/nsidc-0756/versions/3>) which was used in our model has also been downloaded. As shown in **Figure 8**, the bathymetry of ETOPO 1, FOAM and BedMachine all show a shallow trench near 106°W, which is far from the deep trough. It is worth noting that due to the differences in small-scale topography features in the channel, the CDW intrusion on the continental shelf here is questionable in the reanalysis results, but its impact on cross-shelf CDW

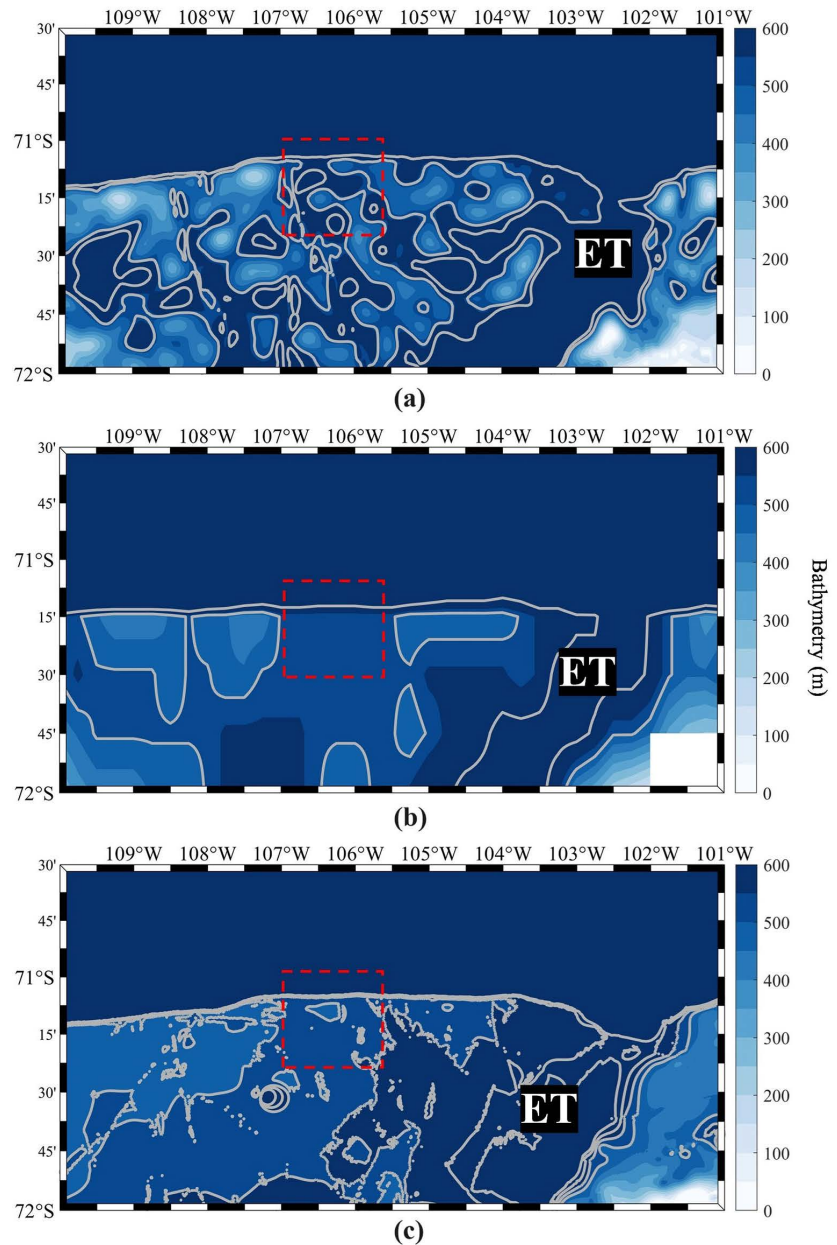


Figure 8. The bathymetry of (a) ETOPO1, (b) FOAM and (c) BedMachine in the SA (red dashed box) and its vicinity. Gray lines represent 700 m and 530 m contours of depth in (a), 700 m and 500 m contours of depth in (b) and 700 m, 600 m, 550 m and 500 m contours of depth in (c).

intrusion is not significant. Thus, the intrusion site at SA near 106°W is reasonable. However, limited by observations, there are still many gaps in our understanding of this region, and more observations are needed to further study CDW intrusion here.

5. Conclusion

In this study, an unreported CDW intrusion site in shallow area (SA) near 106°W away from the deep troughs was found in the WOD data, which has the high-temperature and high-salinity signal near the shelf break. In order to verify the ability of cross-shelf break CDW transport at this site, the numerical particle tracking experiments were implemented at depth 300 m and 400 m. The results indicated that there was indeed an intrusion pathway and a clear tendency of southward CDW transport on the shelf. Through the comparison of heat transport between sections of SA and CT, it was further discovered that CDW intrusion in SA cannot be ignored, because the heat contribution in SA is of the same magnitude as that in CT and even higher in year 2016-2019; during which the mean temperature transport in SA is 3.9 multiples of that in CT. Then the response of CDW intrusion in SA was predicted with the global climate change. We designed a numerical experiment to simulate climate change based on varying wind fields, and the comparison results between control group Test 0 and Test 1 showed that the intrusion in SA is nearly constant; but the intrusion in CT is sensitive to the variations of westerly winds, which indicate that the mechanisms of CDW intrusion may be different in SA and deep troughs. As the cross-isobath intrusion on the slope is related to the topography, we discussed the results of three bathymetry data, ETOPO 1, bathymetry in FOAM and Bed-Machine. All bathymetric data show similar results, with a shallow trench away from the deep troughs near 106°W, which further confirms the existence of this unreported CDW intrusion site. We hope that this study could add to the description of CDW intrusion in Amundsen Sea and draw attention to shallow areas. Due to the lack of observations, current understanding of CDW intrusion in shallow areas near the shelf break is still lacking, and further exploration requires more observational products.

Acknowledgements

We would like to thank Yisen Zhong, Shuangzhao Li and Zhaoru Zhang for their comments and suggestions in this study.

Conflicts of Interest

The authors declare no conflicts of interest regarding the publication of this paper.

References

Armitage, T. W. K., Kwok, R., Thompson, A. F., & Cunningham, G. (2018). Dynamic Topography and Sea Level Anomalies of the Southern Ocean: Variability and Teleconnections.

Journal of Geophysical Research: Oceans, 123, 613–630.

<https://doi.org/10.1002/2017JC013534>

- Assmann, K. M., Jenkins, A., Shoosmith, D. R., Walker, D. P., Jacobs, S. S., & Nicholls, K. W. (2013). Variability of Circumpolar Deep Water Transport onto the Amundsen Sea Continental Shelf through a Shelf Break Trough. *Journal of Geophysical Research: Oceans*, 118, 6603–6620. <https://doi.org/10.1002/2013JC008871>
- Azaneu, M., Webber, B., Heywood, K. J., Assmann, K. M., Dotto, T. S., & Abrahamsen, E. P. (2023). Influence of Shelf Break Processes on the Transport of Warm Waters onto the Eastern Amundsen Sea Continental Shelf. *Journal of Geophysical Research: Oceans*, 128, e2022JC019535. <https://doi.org/10.1029/2022JC019535>
- Boyer, T. P., Baranova, O. K., Coleman, C., Garcia, H. E., Grodsky, A., Locarnini, R. A., et al. (2018). *World Ocean Database 2018*. Version NOAA Atlas NESDIS 87. https://www.ncei.noaa.gov/sites/default/files/2020-04/wod_intro_0.pdf
- Haidvogel, D. B., Arango, H., Budgell, W. P., Cornuelle, B. D., Curchitser, E., Di Lorenzo, E., et al. (2008). Ocean Forecasting in Terrain-Following Coordinates: Formulation and Skill Assessment of the Regional Ocean Modeling System. *Journal of Computational Physics*, 227, 3595–3624. <https://doi.org/10.1016/j.jcp.2007.06.016>
- Holland, P. R., Bracegirdle, T. J., Dutrieux, P., Jenkins, A., & Steig, E. J. (2019). West Antarctic Ice Loss Influenced by Internal Climate Variability and Anthropogenic Forcing. *Nature Geoscience*, 12, 718–724. <https://doi.org/10.1038/s41561-019-0420-9>
- Jacobs, S. S., Hellmer, H. H., & Jenkins, A. (1996). Antarctic Ice Sheet Melting in the Southeast Pacific. *Geophysical Research Letters*, 23, 957–960.
- Kim, T. W., Yang, H. W., Dutrieux, P., Wählin, A. K., Jenkins, A., Kim, Y. G., et al. (2021). Interannual Variation of Modified Circumpolar Deep Water in the Dotson–Getz Trough, West Antarctica. *Journal of Geophysical Research: Oceans*, 126, e2021JC017491. <https://doi.org/10.1029/2021JC017491>
- Lars, B., & Isabella, R. (2021). Classifying Oceanographic Structures in the Amundsen Sea, Antarctica. *Geophysical Research Letters*, 48, e2020GL089412. <https://doi.org/10.1029/2020GL089412>
- Nakayama, Y., Menemenlis, D., Zhang, H., Schodlok, M., & Rignot, E. (2018). Origin of Circumpolar Deep Water intruding onto the Amundsen and Bellingshausen Sea continental shelves. *Nature communications*, 9, 3403. <https://doi.org/10.1038/s41467-018-05813-1>
- Rignot, E., Jacobs, S., Mouginot, J., & Scheuchl, B. (2013). Ice-Shelf Melting Around Antarctica. *Science*, 341, 266–270. <https://doi.org/10.1126/science.1235798>
- Schneider, D. P., Deser, C., & Fan, T. (2015). Comparing the Impacts of Tropical SST Variability and Polar Stratospheric Ozone Loss on the Southern Ocean Westerly Winds. *Journal of Climate*, 28, 9350–9372. <https://doi.org/10.1175/JCLI-D-15-0090.1>
- Shchepetkin, A. F., & McWilliams, J. C. (2005). The Regional Oceanic Modeling System (ROMS): A Split-Explicit, Free-Surface, Topography-Following-Coordinate Oceanic Model. *Ocean Modelling*, 9, 347–404. <https://doi.org/10.1016/j.ocemod.2004.08.002>
- Steig, E. J., Ding, Q., Battisti, D. S., & Jenkins, A. (2012). Tropical Forcing of Circumpolar Deep Water Inflow and Outlet Glacier Thinning in the Amundsen Sea Embayment, West Antarctica. *Annals of Glaciology*, 53, 19–28. <https://doi.org/10.3189/2012AoG60A110>
- Taylor, K. E. (2001). Summarizing Multiple Aspects of Model Performance in a Single Diagram. *Journal of Geophysical Research: Atmospheres*, 106, 7183–7192. <https://doi.org/10.1029/2000JD900719>
- Thoma, M., Jenkins, A., Holland, D., & Jacobs, S. (2008). Modelling Circumpolar Deep

- Water Intrusions on the Amundsen Sea Continental Shelf, Antarctica. *Geophysical Research Letters*, 35, L18602. <https://doi.org/10.1029/2008GL034939>
- Thompson, D. W. J., Solomon, S., Kushner, P. J., England, M. H., Grise, K. M., & Karoly, D. J. (2011). Signatures of the Antarctic Ozone Hole in Southern Hemisphere Surface Climate Change. *Nature Geoscience*, 4, 741-749. <https://doi.org/10.1038/ngeo1296>
- Vaughan, D. G. (2008). West Antarctic Ice Sheet collapse—The Fall and Rise of a Paradigm. *Climatic Change*, 91, 65–79. <https://doi.org/10.1007/s10584-008-9448-3>
- Wåhlin, A. K., Muench, R. D., Arneborg, L., Björk, G., Ha, H. K., Lee, S. H., & Alsén, H. (2012). Some Implications of Ekman Layer Dynamics for Cross-Shelf Exchange in the Amundsen Sea. *Journal of Physical Oceanography*, 42, 1461-1474. <https://doi.org/10.1175/JPO-D-11-041.1>
- Wåhlin, A. K., Yuan, X., Björk, G., & Nohr, C. (2010). Inflow of Warm Circumpolar Deep Water in the Central Amundsen Shelf. *Journal of Physical Oceanography*, 40, 1427-1434. <https://doi.org/10.1175/2010JPO4431.1>
- Walker, D. P., Brandon, M. A., Jenkins, A., Allen, J. T., Dowdeswell, J. A., & Evans, J. (2007). Oceanic Heat Transport onto the Amundsen Sea Shelf through a Submarine Glacial Trough. *Geophysical Research Letters*, 34, L02602. <https://doi.org/10.1029/2006GL028154>
- Walker, D. P., Jenkins, A., Assmann, K. M., Shoosmith, D. R., & Brandon, M. A. (2013). Oceanographic Observations at the Shelf Break of the Amundsen Sea, Antarctica. *Journal of Geophysical Research: Oceans*, 118, 2906-2918. <https://doi.org/10.1002/jgrc.20212>
- Wang, C., Zhang, Z., Zhong, Y., & Zhou, M. (2024). A Model Study of Buoyancy Driven Cross-Isobath Transport over the Ross Sea Continental Shelf Break. *Journal of Geophysical Research: Oceans*, 129, e2023JC020078. <https://doi.org/10.1029/2023JC020078>